Research Article

Power Control for Passive QAM Multisensor Backscatter Communication Systems

Shengbo Hu,[1,2] Jinrong Mo,[1,2] Tingting Yan,[1,2] and Yanfeng Shi[1,2]

[1]Institute of Intelligent Information Processing, Guizhou Normal University, Guiyang 550001, China
[2]Center for RFID and WSN Engineering, Department of Education, Guizhou Normal University, Guiyang 550001, China

Correspondence should be addressed to Jinrong Mo; 935472997@qq.com

To achieve good quality of service level such as throughput, power control is of great importance to passive quadrature amplitude modulation (QAM) multisensor backscatter communication systems. First, we established the RF energy harvesting model and gave the energy condition. In order to minimize the interference of subcarriers and increase the spectral efficiency, then, the colocated passive QAM backscatter communication signal model is presented and the nonlinear optimization problems of power control are solved for passive QAM backscatter communication systems. Solutions include maximum and minimum access interval, the maximum and minimum duty cycle, and the minimal RF-harvested energy under the energy condition for node operating. Using the solutions above, the maximum throughput of passive QAM backscatter communication systems is analyzed and numerical calculation is made finally. Numerical calculation shows that the maximal throughput decreases with the consumed power and the number of sensors, and the maximum throughput is decreased quickly with the increase of the number of sensors. Especially, for a given consumed power of sensor, it can be seen that the throughput decreases with the duty cycle and the number of sensors has little effect on the throughput.

1. Introduction

Since the advent of backscatter communication, it has been widely used in the passive RFID (radio frequency identification) system due to its low cost and low power [1, 2]. Similarly, using the principle of the backscatter communication, the passive sensor node transmitter can be simplified into a transistor connected to the antenna. This will greatly reduce the cost and power consumption of wireless communication systems. For example, scholars from the University of Washington [3] researched the WISP (wireless identification and sensing platform) wireless smart sensor systems which can harvest RF energy based on backscatter communication. Now, PBC (passive backscatter communication) has been applied in these fields of smart car, wireless temperature measurement, the biological signal acquisition [4–9], and so forth. Undoubtedly, the study and application of passive backscatter communication will attract more and more attention.

In passive backscatter communication systems, sensor nodes need to harvest RF energy from the transceivers or reader and use it to recharge their finite energy storage capacity as shown in Figure 1. However, the unpredictable environments such as the channel, the number of sensors, and challenges of the RF energy harvesting make the activities of the sensors difficult, including sensing, processing, and communicating by nodes with a given rate. So, an efficient energy management is necessary in order to guarantee sensors' activities and a QoS (quality of service) of backscatter communication [10–12].

In fact, the mode using RF energy harvesting as a supplement to the finite energy storage capacity is called energy neutral operation [13]. In this mode, for such RF energy harvesting nodes with ideal finite energy storage capacity, the condition for energy neutral operation should be satisfied for all nonnegative values of τ:

$$\int_0^\tau P_c(t)dt \leq \int_0^\tau P_{RF}(t)dt + B_0, \quad (1)$$

where $P_{RF}(t)$ is the harvested RF power at time t, $P_c(t)$ is the consumed power by nodes at that time, B_0 is the initial
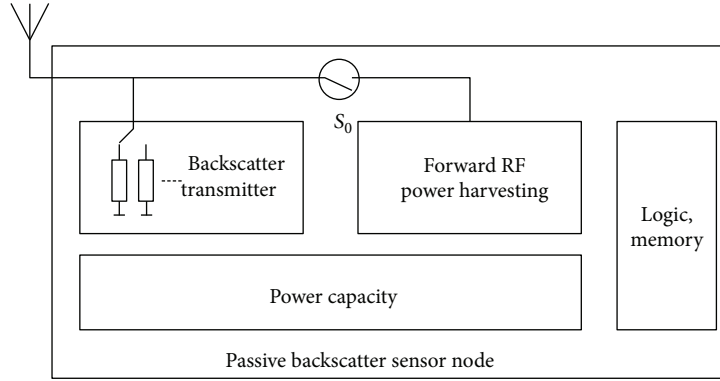
FIGURE 1: Passive backscatter sensor node.

energy stored in the ideal capacity, and τ is the runtime. So, the goal of power control for passive backscatter communication is to maximize QoS level under condition of energy neutral operation.

For implementing multisensor backscatter communication systems, subcarrier modulation can be used for each sensor [14]. This leads to interference among sensors. In order to minimize such interference and increase spectral efficiency, modulations including QAM are used to improve data throughput [15–17]. It shows that it is feasible to use load-dependent scattering for yielding a simple QAM backscatter [15, 17]. In this paper, we focus on colocated multisensor QAM backscatter communication, showing that power control is important for the backscatter communication systems to achieve good QoS level via analysis and simulation. We introduce a related work in Section 2 and describe a system model in Section 3. In Section 4, we present the performance of the backscatter communication systems. And we analyze the impact of power control on the throughput of systems in Section 5. Finally, we provide some concluding remarks in Section 6.

2. Related Work

Several papers have mainly proposed power control on nodes using energy harvesting, because power control of energy harvesting determines the level of connectivity of backscatter communication as well as the achievable QoS of the systems. An RF-powered transmitter that supports 915 MHz downlink and 2.45 GHz uplink bands is designed in [18]. In [19], the paper computes the minimal number of sinks required to keep the network connected and to satisfy the required constraints.

There exist attractive applications of the RF-powered devices such as wireless body networks. Benefiting from RF energy harvesting, some low-power devices can achieve real-time work-on-demand power from RF sources, which further enables a battery-free circuit with reduced size [20]. The body devices that implement high efficiency can be found in [21, 22]. For the multisensor system, we can refer [23]. The authors address the problem of developing energy-efficient transmission strategies for body sensor networks with energy harvesting [24]. And the authors evaluate the impact of transmit power control on the

usefulness of a multisink WSN-Heap using energy harvesting, deployed in uniform string topology for railway track monitoring [25].

3. System Models

3.1. RF Energy-Harvesting Model. The RF energy harvester is composed of an antenna, impedance matching circuit, rectifier, and voltage multiplier as shown in Figure 2. The efficiency η of the RF energy harvester is defined as follows:

$$\eta = \eta_1 \eta_2 \eta_3 = \frac{P_{\text{eh}}}{P_{\text{in}}}, \qquad (2)$$

where η_1, η_2, and η_3 are the efficiencies of the receiving antenna, impedance transformation network, and the rectifier, respectively, P_{eh} is the output DC power and the meaning of eh is energy harvesting, and P_{in} is the input RF power.

In Figure 2, Y-stage voltage multiplier circuits are used to promote the output voltage. So, the upper limit of the steady-state output voltage V_{dd} is increased by a factor Y and can be written as [26]

$$V_{\text{dd}} = 2Y \left(V_{\text{peak}} - V_{\text{on}} \right), \qquad (3)$$

where V_{peak} is the peak voltage of the signal at the input of the view of the Y-stage voltage multiplier circuits and V_{on} is the turn-on voltage of the diode.

Now, let us consider the minimum voltage for nodes to operate. Assuming, the harvesting power from the transceivers or reader is $P_{\text{eh}}(t)$ and the consumed power by nodes at that time is $P_{\text{c}}(t)$. When the power made available by the transceivers or reader is insufficient for continuous operation, that is, $P_{\text{eh}}(t) < P_{\text{c}}(t)$, a capacity must be used to store RF energy until enough RF energy exists to complete an access. This affects the backscatter communication QoS level. Under these circumstances, the capacitor must be charged unless the stored energy E_{stored} is greater than or equal to the access energy E_{access}, where E_{access} is the energy required for each access.

The stored energy E_{stored} can be written as

$$E_{\text{stored}} = \frac{1}{2} C \left(V_{\text{dd}}^2 - V_{\text{node}}^2 \right), \qquad (4)$$
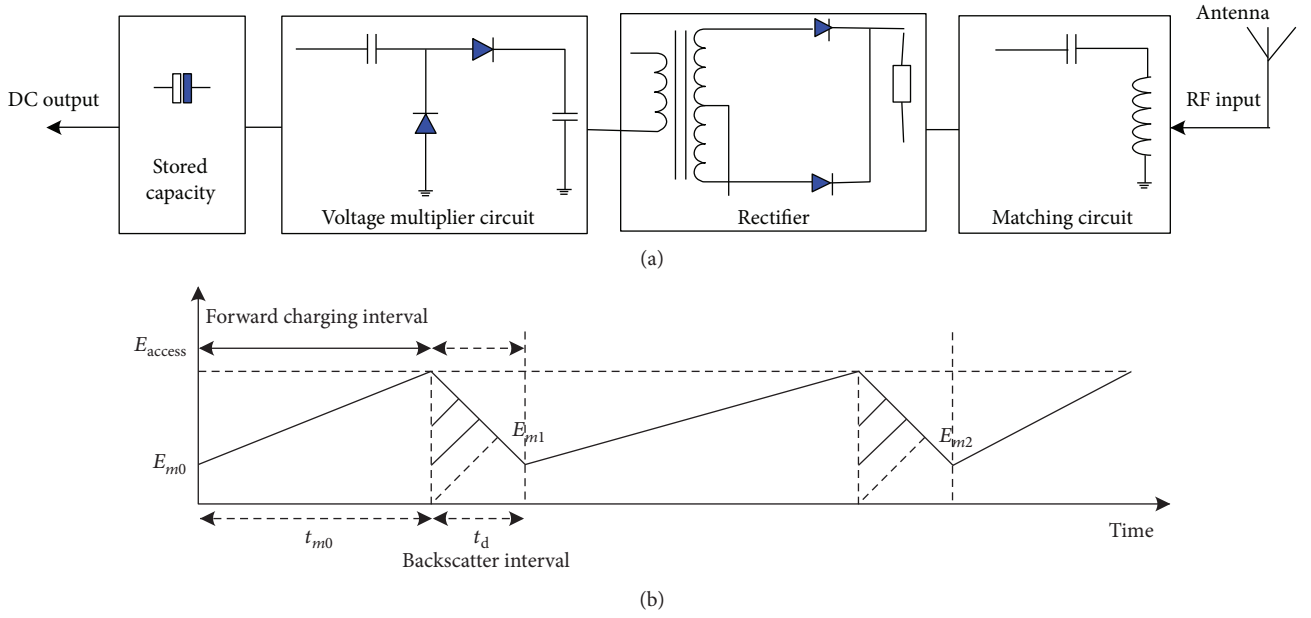
FIGURE 2: RF energy-harvesting model.

where C is the value of energy harvesting circuit output capacity and V_{node} is the voltage level at which the node operates. And the access energy E_{access} can be written as

$$E_{access} = \int_{T_0}^{T_0+T_{access}} P_c dt = V_{node} \int_{T_0}^{T_0+T_{access}} I_{access} dt, \quad (5)$$

where $[T_0, T_0 + T_{access}]$ is the access interval and I_{access} is the time-varying current draw of the node during each access.

Hence, the minimum voltage for nodes to operate is solved as

$$V_{dd}^{min} = \sqrt{\left(\frac{2E_{access}}{C}\right) + V_{node}^2}. \quad (6)$$

Once $V_{dd} < V_{dd}^{min}$, the node can not operate.

3.2. Energy Condition for Node Operating. Backscatter communication links include forward link and backscatter link. While accessing, the node harvests RF energy from the transceivers or reader firstly by forward link. Once $V_{dd} \geq V_{dd}^{min}$, that is, $E_{stored} \geq E_{access}$, the node draws power to carry out its operation and sends the sensor data to the transceivers or reader by backscatter link. These can be defined as an energy model as given in Figure 2. Each access interval comprises a charging phase and backscatter communication phase. In Figure 2, while accessing at time T_0, the capacitor C charges unless the stored energy is $E_{stored} \geq E_{access}$ at time $T_0 + T_c$. Then, the node sends data by backscatter link. Once $E_{stored} < E_{access}$ at time $T_0 + T_c + T_d$, the node stops operating and waits next access. Let $E_{eh} = B_0 + \eta \int_{T_0}^{T_0+T_c} [P_{eh}(t) - P_c(t)]^+ dt$, the condition for energy

neutral operation should be satisfied in the access interval $[T_0, T_0 + T_{access}]$:

$$E_{eh} - \int_{T_0+T_c}^{T_0+T_c+T_d} [P_c(t) - P_{eh}(t)]^+ dt \geq 0, \quad (7)$$

where $\eta \in [0, 1]$ is the charging rate, B_0 is the initial energy stored in the capacity, and the rectifier function $[x]^+$ is defined as follows:

$$[x]^+ = \begin{cases} x, & x \geq 0, \\ 0, & x < 0. \end{cases} \quad (8)$$

Meanwhile, the limitation of capacity size requires the constraint to be satisfied as follows:

$$E_{eh} - \int_{T_0+T_c}^{T_0+T_c+T_d} [P_c(t) - P_{eh}(t)]^+ dt \leq B, \quad (9)$$

where B is the maximum energy that can be stored in the capacitor.

Hence, the energy conditions for the node operating include (7), (9), and (10). And (10) is given as follows:

$$B_0 + \eta \int_{T_0}^{T_0+T_c} [P_{eh}(t) - P_c(t)]^+ dt \geq E_{task}, \quad (10)$$

where E_{task} is the minimum energy required for the node to operate.

For simplicity, assuming the consumed power by the node with forward link is P_{fc}, the consumed power by the sensor with backscatter link is $P_{bc}(P_{fc} < P_{bc})$ and P is
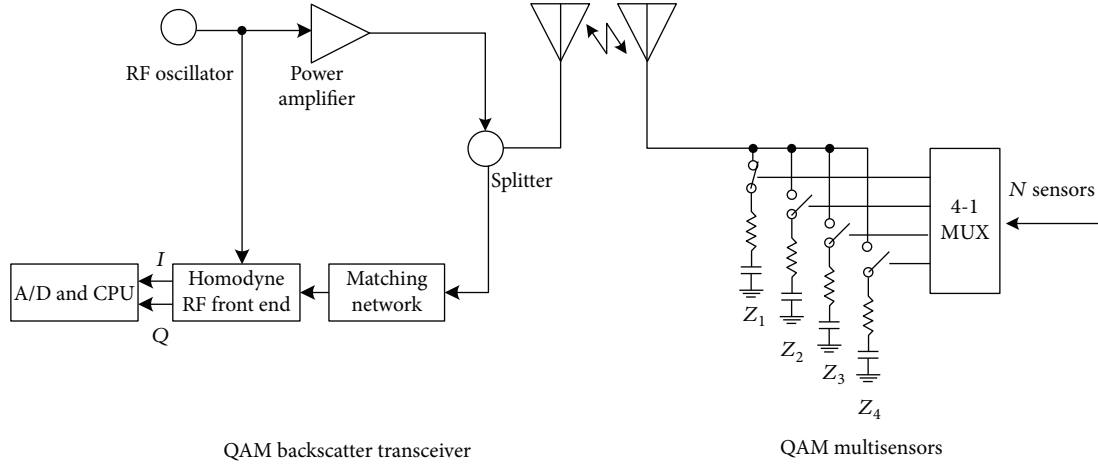
Figure 3: Passive QAM backscatter multisensor communication systems.

the harvested power, then the energy condition for node operating is given as follows:

$$
\begin{aligned}
B_0 + \eta T_c (P - P_{fc}) - T_d P_{bc} &\geq 0, \\
B_0 + \eta T_c (P - P_{fc}) - T_d P_{bc} &\leq B, \\
B_0 + \eta T_c (P - P_{fc}) &\geq E_{access}.
\end{aligned}
\tag{11}
$$

4. Performance Analysis

4.1. Colocated QAM Multisensor Backscatter Signal. Typically, backscatter communication systems use single-frequency continuous wave transmission waveforms for accessing. The resulting complex signal from the node received at the transceivers or reader is given as

$$
r(t) = \sqrt{2E\alpha} m(t) \exp[j(\omega_c t + \varphi)] + n(t), \tag{12}
$$

where E, ω_c, and φ are the peak power, the angular frequency, and the phase of the carrier signal, respectively, $n(t)$ is AWGN (additive white Gaussian noise), and $m(t)$ is the message signal to be transmitted.

To improve spectral efficiency, the use of QAM opens up many new avenues for backscatter communication systems. It has been shown recently that it is feasible to build backscatter systems supporting QAM using node load selection methodology [17, 27]. However, improved spectral efficiency means that the node's impedance is mismatched and the power harvested or the efficiency of impedance transformation network η_2 is reduced.

What is more, $m(t)$ can be given as

$$
m(t) = \sum_{k=-\infty}^{\infty} a_k g(t - kT), \tag{13}
$$

where $g(t)$ is the rectangle pulse with width T and $\{a_k\}$ is the sequence of symbols with L levels. If the number of phases φ is K in (12), the number of the carrier states is $K \times L$. And when $K = L = 2$, the modulation is 4QAM, that is, to design and implement 4QAM backscatter modulator,

four RC lumped impedances are connected to an antenna port through RF 4-1 Mux, each lumped impedance corresponding to different reflection coefficients. The design of 4QAM colocated backscatter communication systems with this procedure is given in Figure 3. In Figure 3, serial/parallel converts sensor data into 2 bits for controlling the 4-1 Mux.

To make the structure of the backscatter multisensor nodes simple, we put forward an access scheme with different subcarrier modulations for each sensor; namely, each sensor has different pulse width. So, the cumulative colocated QAM multisensor backscatter signal at the transceivers or reader is a sum of all complex signals from sensors with additive white noise, resulting in

$$
\begin{aligned}
r(t) = &\sqrt{2P_i \alpha_i} m_i(t) \exp[j(\omega_c t + \varphi)] \\
&+ \sum_{k \neq i} \sqrt{2P_k \alpha_k} m_k(t) \exp[j(\omega_c t + \varphi)] + n(t).
\end{aligned}
\tag{14}
$$

4.2. Throughput Maximization for Colocated QAM Multisensor under the RF Energy-Harvesting Constraints. The goal of power control for passive multisensor random interrogating is to meet some QoS criteria, for example, throughput.

In Figure 3, each sensor has different subcarrier frequencies; however, the information leak of one sensor interferes other sensors. The amount of such interference depends on the power spectrum of the chosen subcarrier modulation and the number of sensors. According to the constraint of the correlated short-range wireless communication spectrum, the power spectrum of QAM modulation of the ith sensor can be approximated as [28]

$$
S(f) \approx \frac{1}{(f - f_i)^4}, \tag{15}
$$

where $f_i = 1/T_i$ and T_i is the pulse width of the ith sensor data.

Under the lognormal channel, signal-to-interference-and-noise ratio (SINR) at the transceivers or reader in Figure 3 is written as

$$\Gamma_i = \frac{2E_i h_i}{(W_0/T_i) + \sum_{j=1, \neq i}^{N} 2E_j h_j S\left(f_j - f_i\right)}, \qquad (16)$$

where E_i is the transmitted bit energy, W_0 is the power spectrum density, $h_i = l_i \Omega_i$, l_i is the path loss, Ω_i is the shadow fading of logarithmic normal distribution, and $\Omega_i = e^x$. x follows normal distribution $G(\mu, \sigma^2)$.

In this paper, the multiple sensors are colocation and share a transmitter and transceiver, so it can be assumed that $h_i = h_j$ and $E_i = E_j$. Consequently, (16) can be rewritten as

$$\Gamma_i = \frac{1}{\Gamma_N^{-1} + \Gamma_I^{-1}}, \qquad (17)$$

where $\Gamma_N = 2E_i T_i \cdot l_i^{\gamma_i} \cdot 10^{x_i/10}/W_0$ and $\Gamma_I = \sum_{j=1, \neq i}^{N} 10^{(x_i - x_j)/10} \cdot (l_i/l_j)^{\gamma} \cdot (1/(S(f_j - f_i)))$.

Now, we characterize the performance of backscatter communication. We start by defining the concept of the throughput.

Definition 1. The data delivery ratio D_r of backscatter communication systems is a ratio of successful data packet received to attempted data packet transmitted.

Definition 2. The throughput T_h of backscatter communication systems is the probability that a packet is successfully received during a data interrogation interval.

For a packet to be received successfully, the SINR at the transceivers or reader must exceed some threshold λ_{th}. Using the definitions above, the data delivery ratio D_{ri} and the throughput T_{hi} in the access interval T_{access} of the ith sensor can be written, respectively, as

$$D_{ri} = P\{\Gamma_i \geq \lambda_{th}\},$$
$$T_{hi} = \frac{P\{\Gamma_i \geq \lambda_{th}\}}{T_{access}}. \qquad (18)$$

So, the average data delivery ratio and throughput of the backscatter communication systems can be written as follows:

$$D_r = \frac{\sum_{i=1}^{N} D_{ri}}{N},$$
$$T_h = \frac{\sum_{i=1}^{N} T_{hi}}{N}, \qquad (19)$$

where N is the number of sensors.

Generally, obtaining throughput in a closed form is not always possible and remains analytically challenging; because of the cumulative distribution function of random variable, Γ_i remains difficult. Thanks to nodes colocating, this problem

can be solved easily. In this case, $x_i = x_j$, $l_i = l_j$, and (16) can be rewritten as

$$\Gamma_i = \frac{1}{\Gamma_N^{-1} + \sum_{j=1, \neq i}^{N} S\left(f_j - f_i\right)}. \qquad (20)$$

Let

$$k_i = 10\log\left(\frac{W_0}{2E_i T_i l_i^{\gamma_i}} \cdot \frac{\lambda_{th}}{1 - \lambda_{th}\sum_{j=1, \neq i}^{N} S\left(f_j - f_i\right)}\right), \qquad (21)$$

then,

$$D_{ri} = P\{\Gamma_i \geq \lambda_{th}\} = P\{x_i \geq k_i\}$$
$$= 1 - P(x_i < k_i) = 1 - \int_{-\infty}^{k_i} \frac{1}{\sqrt{2\pi}\sigma_i} e^{-\left(x_i^2/2\sigma_i^2\right)} dx. \qquad (22)$$

Hence, the average data throughput T_h can be rewritten as

$$T_h = \frac{\sum_{i=1}^{N} D_{ri}}{N T_{access}} = \frac{\sum_{i=1}^{N}\left(1 - \int_{-\infty}^{k_i}\left(1/\sqrt{2\pi}\sigma_i\right) e^{-\left(x_i^2/2\sigma_i^2\right)} dx\right)}{N T_{access}}. \qquad (23)$$

Assuming duty cycle $\rho = \bar{T}_d/(\bar{T}_c + \bar{T}_d) = \bar{T}_d/\bar{T}_{task}$, $\rho \in [0, 1]$, the nonlinear optimization problems of power control for passive QAM backscatter communication systems with N nodes can be expressed as

$$\max T_h = \frac{\sum_{i=1}^{N} D_{ri}}{N T_{access}}, \qquad (24)$$

subject to

$$B_{0m} + \eta(1 - \rho)\bar{T}_{task}(P - NP_{fc}) - \rho N \bar{T}_{task} P_{bc} \geq 0,$$
$$B_{0m} + \eta(1 - \rho)\bar{T}_{task}(P - NP_{fc}) - \rho N \bar{T}_{task} P_{bc} \leq B,$$
$$B_{0m} + \eta(1 - \rho)\bar{T}_{task}(P - NP_{fc}) \geq E_{task},$$
$$B_0 \leq B. \qquad (25)$$

5. Numerical Results and Discussions

We evaluate the performance of the power control using numerical analysis. The analysis includes the impact of P_{bc} on the throughput and the harvested power.

5.1. Parameters for Numerical Analysis. Referring to the relation between bit error rate and SINR for 4QAM under AWGN channel, the threshold λ_{th} can be chosen as 3.0156 corresponding to the data delivery ratio ranging from 1 to 1×10^{-5}. Meanwhile, the given transmission data rate is 40 kbps, the data packet size is 64 bits, and the duration of a data packet transmission is $T_{dm} = 1.6$ sec. All parameters used are listed in Table 1 [29].

5.2. Impact of P_{bc} on Throughput T_h. In this section, we first investigate the choice of P_{bc} to achieve maximal throughput.

TABLE 1: Parameters for numerical analysis.

Parameter	Value
W_0	−1.0779 dBw/Hz
l_i	−1 dB
λ_{th}	3.0156
T_{dm}	1.6 sec
P_{fc}	68.9 nW
B	0.0125 J
η	0.65

Under the energy condition for node operating in (11) and solving the inequality group, it can be shown that the maximum and minimum access interval T_{access} is given by

$$T_{access}^{min} = \frac{\eta T_d(P - NP_{fc}) + NT_dP_{bc}}{\eta(P - NP_{fc})},$$

$$T_{access}^{max} = \frac{\eta T_d(P - NP_{fc}) + NT_dP_{bc} + B}{\eta(P - NP_{fc})}. \tag{26}$$

The access interval T_{access} is a function of P_{bc}. When $P = 189\,\mu W$, $N = 2$, $N = 4$, and $N = 8$, the minimum and maximum access intervals of sensor node1 with subcarrier $f_1 = 50000\,Hz$ are plotted in Figures 4 and 5. The subcarriers of other nodes are 50,002 Hz, 50,010 Hz, 50,100 Hz, 50,110 Hz, 50,120 Hz, 50,150 Hz, and 50,200 Hz (the same below). According to these frequencies and the value of T_{access}, we can deduce the corresponding value of the throughput using (20), (23), and (24). And the throughput changes by varying of T_{access}.

It is observed that the maximum and minimum access intervals T_{access} increase with P_{bc} in Figures 4 and 5. It is easy to understand, because the greater the P_{bc}, the longer the charge time to meet the energy condition for node operating. It is worthwhile to note that the maximum and minimum access interval T_{access} increases more with the increase of N.

Hence, the maximum throughput as a function of P_{bc} is plotted under the condition of the minimum access interval T_{access} in Figure 6. It is found that the maximal throughput decreases with the increase of P_{bc}. And the maximum throughput is decreased quickly with the increase of N.

5.3. Impact of Duty Cycle ρ on Throughput T_h. Next, we investigate the impact of varying duty cycle ρ on the throughput T_h.

Similar to Section 4.2, the maximum and minimum duty cycle ρ under the energy condition for node operating is given as follows:

$$\rho_{max} = \frac{\eta T_d(P - NP_{fc})}{\eta T_d(P - NP_{fc}) + NT_dP_{bc}},$$

$$\rho_{min} = \frac{\eta T_d(P - NP_{fc})}{B + \eta T_d(P - NP_{fc}) + NT_dP_{bc}}. \tag{27}$$

For a given $P_{bc} = 0.524\,\mu W$ and a given $P_{fc} = 0.0689\,\mu W$, the throughput T_h as a function of duty cycle ρ is shown in
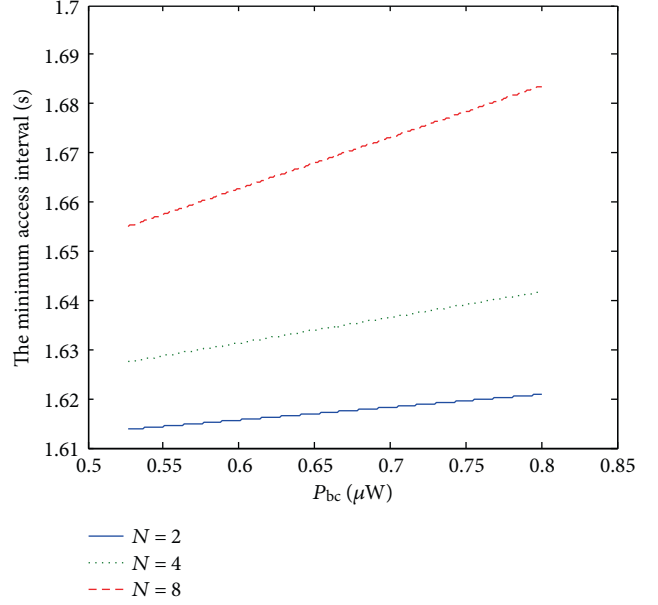

FIGURE 4: The minimum access interval versus the consumed power by sensor with scatter link.
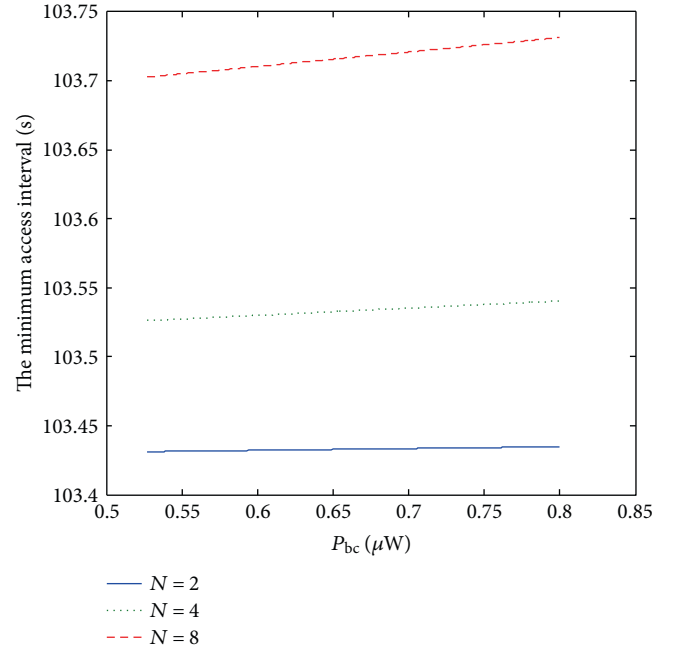

FIGURE 5: The maximum access interval versus the consumed power by sensor with scatter link.

Figure 7. It can be seen that the throughput T_h decreases with the increase of duty cycle ρ. Because decreasing duty cycle ρ leads to the increasing of the access interval T_{access}.

It should be noted that N has little effect on the throughput in Figure 7, because duty cycle ρ is insensitive to N. Especially, N has almost no effect on the minimum duty cycle ρ. We can analyze this using parameter sensitivity.
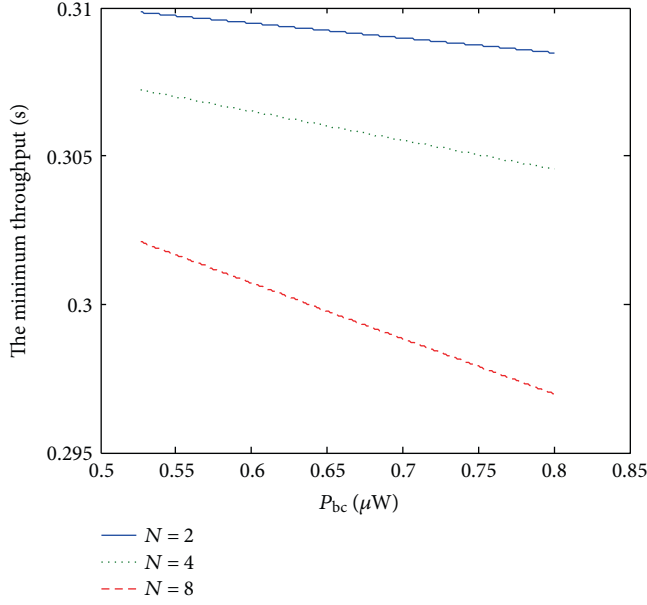
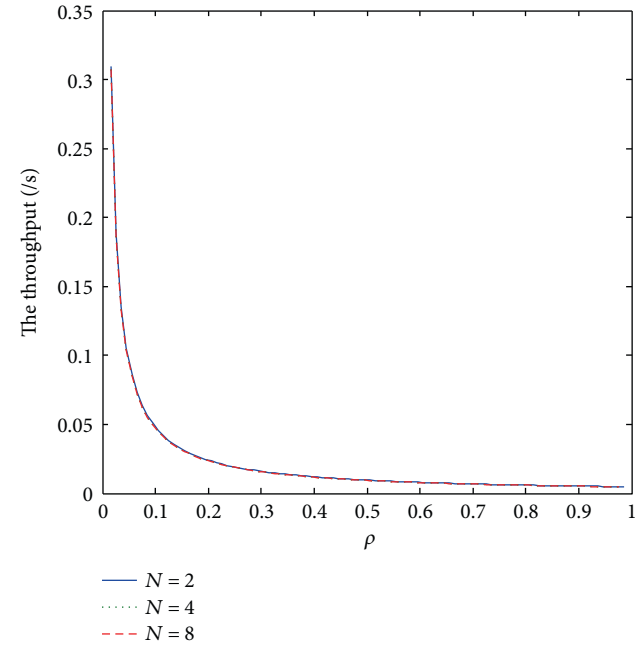Figure 6: The maximum throughput versus the consumed power by sensor with scatter link.

Figure 7: The throughput versus the duty cycle ρ.

Figure 8: The sensitivity of duty cycle about N.
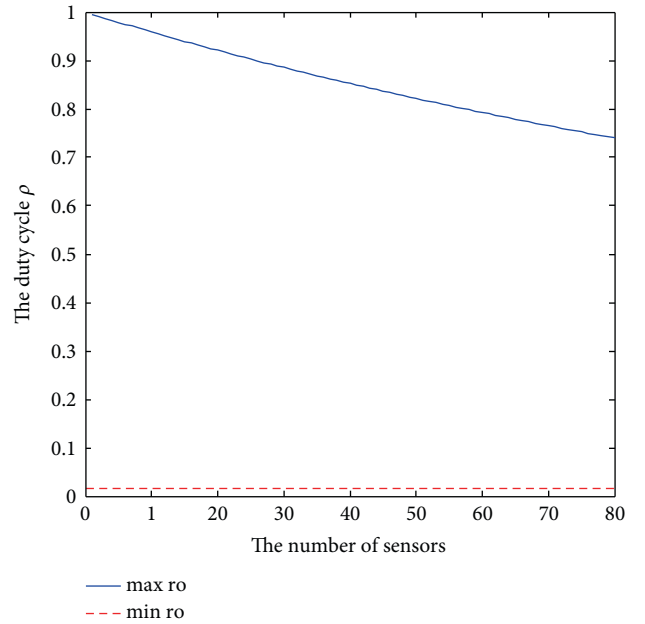
Figure 9: The relation between the duty cycle ρ and N.

Taking the partial derivative, the sensitivity of ρ_{max} and ρ_{min} is given as

$$
\begin{aligned}
S_{\rho_{max}} &= \left| \frac{\partial \rho_{max}}{\partial N} \right| = \frac{\eta T_d^2 P P_{bc}}{\left[\eta T_d (P - N P_{fc}) + N T_d P_{bc} \right]^2}, \\
S_{\rho_{min}} &= \left| \frac{\partial \rho_{min}}{\partial N} \right| = \frac{\eta \left(T_d^2 P P_{bc} + T_d B P_{fc} \right)}{\left[B + \eta T_d (P - N P_{fc}) + N T_d P_{bc} \right]^2}.
\end{aligned}
\tag{28}
$$

Hence, the $S_{\rho_{max}}$ and $S_{\rho_{min}}$ as functions of N are shown in Figure 8. In Figure 8, $S_{\rho_{max}}$ and $S_{\rho_{min}}$ are very small. Especially, N has almost no effect on the minimum duty cycle ρ, because of using the large stored capacity. This can be also seen from the relation between duty cycle ρ and N shown in Figure 9.

5.4. Impact of P_{bc} on the Minimum Harvested Energy P_{min}. Finally, we analyze the choice of P_{bc} to achieve
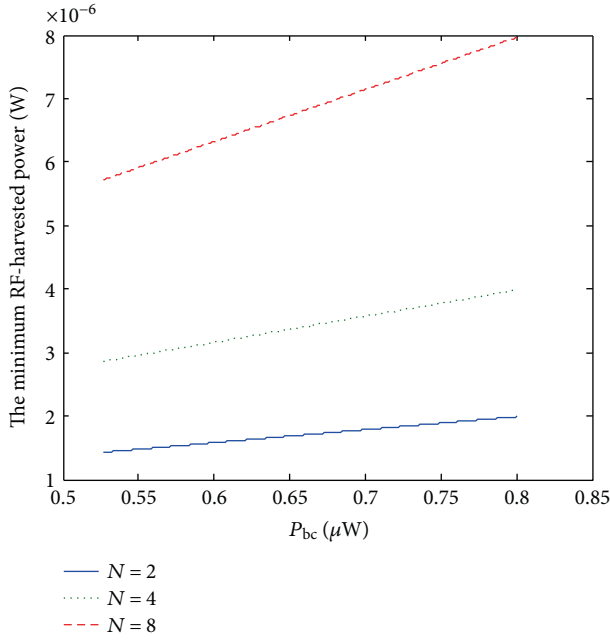
FIGURE 10: The minimum RF-harvested power versus the consumed power by sensor with scatter link.

the minimal RF-harvested energy under the energy condition for node operating.

In the same way, we can derive that the minimal RF-harvested energy is given by

$$P_{\min} = NP_{bc} + \frac{E_{task}}{\eta(1 - \rho)T_{task}}. \tag{29}$$

The $P_{\min}$ as a function of P_{bc} is plotted in Figure 10. In Figure 10, as the P_{bc} and N increase, the $P_{\min}$ increases. This conclusion is obvious. Similar to Section 5.2, the number of sensors has larger effect on the minimum RF-harvested power.

6. Conclusion

To achieve good QoS level such as throughput, power control is of great importance to passive QAM multisensor backscatter communication systems. This paper presents the RF energy-harvesting model and gives the energy condition for node operating. In order to minimize interference resulted from multisensors and increase spectral efficiency, we propose the colocated passive QAM backscatter communication signal model, give the closed-form solution of the throughput under log-normal channel, and put forward the nonlinear optimization problems of power control for passive QAM backscatter communication systems. Solving the nonlinear optimization problems, we obtain the maximum and minimum access intervals, the maximum and minimum duty cycle, and the minimal RF harvested energy under the condition of node operating. Based on the solutions above, we analyze the maximum throughput of passive QAM

backscatter communication systems and make numerical calculation. Finally, we make the conclusion as follows:

(i) The energy condition for node operating is a prerequisite for designing and optimizing the passive backscatter communication systems, and the goal of power control is to maximize the QoS of the systems.

(ii) Under the energy condition for node operating, the consumed power P_{bc} of the sensor with backscatter link and the number of sensors has large effect on the throughput of systems. It is found that the maximal throughput decreases with the increase of P_{bc} and N and the maximum throughput is decreased quickly with the increase of N.

(iii) Especially, for a given P_{bc} and a given P_{fc}, it can be seen that the throughput T_h decreases with the increase of duty cycle ρ and the number of sensors has little effect on the throughput.

(iv) There also exists a further improvement in this paper. For the next phase work, we will try to establish an actual model for data measurement and we will consider the WCDMA or LTE signals substituting for QAM signals.

Conflicts of Interest

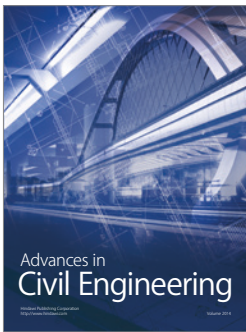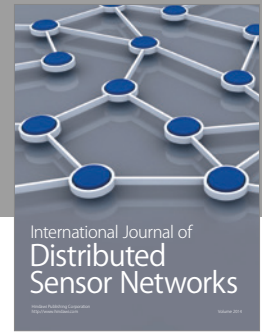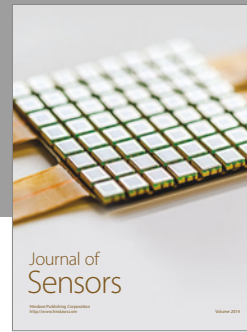The authors declare that they have no conflicts of interest.

Acknowledgments

References

[1] H. Stockman, "Communication by means of reflected power," *Proceedings of the IRE*, vol. 36, no. 10, pp. 1196–1204, 1948.

[2] A. Sample, D. Yeager, and P. Powledge, "Design of an RFID-based battery-free programmable sensing platform," *IEEE Transactions on Instrumentation and Measurement*, vol. 57, no. 11, pp. 2608–2615, 2008.

[3] D. Yeager, F. Zhang, and A. Zarrasvand, "A 9μA, addressable Gen2 sensor tag for biosignal acquisition," *IEEE Journal of Solid-State Circuits*, vol. 45, no. 10, pp. 2198–2209, 2010.

[4] W. U. Bajwa, A. Sayeed, and R. Nowak, "Matched source-channel communication for field estimation in wireless sensor networks," in *Proceedings of Information Processing in Sensor Networks, 2005*, Los Angeles, CA, USA, April 2005.

[5] S. Ergen, A. S. Vincentelli, and X. Sun, "The tire as an intelligent sensor," *IEEE Transaction on Computer-Aided Design of Integrated Circuits and Systems*, vol. 28, no. 7, pp. 941–955, 2009.

[6] J. Grosinger, "Feasibility of backscatter RFID systems on the human body," *EURASIP Journal on Embedded Systems*, vol. 2013, no. 1, pp. 1–10, 2013.

[7] S. Hu, S. Bing, and S. Heng, "Power transmission performance for ultra high frequency embedded RFID system in tire," *Transactions of the Chinese Society of Agricultural Engineering*, vol. 29, no. 21, pp. 150–158, 2013.

[8] P. V. Bharat, N. Sihna, and K. E. Pujitha, "Tire pressure monitoring system using ambient backscatter technology containing RF harvesting circuitry," *International Journal of Advance Engineering and Research Development*, vol. 1, no. 6, pp. 1–11, 2014.

[9] P. Ferrari, A. Flammini, and E. Sisinni, "New architecture for a wireless smart sensor based on a software defined radio," *IEEE Transaction on Instrumentation and Measurement*, vol. 60, no. 6, pp. 2133–2141, 2011.

[10] A. Kansal, D. Potter, and M. B. Srivastava, "Performance aware tasking for environmentally powered sensor networks," in *Proceedings of ACM SIGMETRICS*, vol. 32, no. 1, pp. 223–234, New York, NY, USA, 2006.

[11] H. Yoo, M. Shim, and D. Kim, "Self-synchronized and energy-aware duty cycle control algorithm in energy-harvested wireless sensor networks," *IEEE Communications Letters*, vol. 16, no. 2, pp. 203-204, 2012.

[12] L. Varga, G. Romaniello, and M. Favre, "GreenNet: an energy-harvesting IP-enabled wireless sensor network," *IEEE Internet of Things Journal*, vol. 2, no. 5, pp. 412–426, 2015.

[13] A. Kansal, J. Hsu, and S. Zahedi, "Power management in energy harvesting sensor networks," *ACM Transactions on Embedded Computing Systems*, vol. 6, no. 4, pp. 1–35, 2007.

[14] M. Z. Win, P. C. Pinto, and L. A. Shepp, "A mathematical theory of network interference and its applications," *Proceedings of the IEEE*, vol. 97, no. 2, pp. 205–230, 2009.

[15] A. Bletsas, A. G. Dimitriou, and J. N. Sahalos, "Improving backscatter radio tag efficiency," *IEEE Transaction on Microwave Theory and Techniques*, vol. 58, no. 6, pp. 1502–1509, 2010.

[16] H. Ju and R. Zhang, "Throughput maximization in wireless powered communication networks," *IEEE Transactions on Wireless Communications*, vol. 13, no. 1, pp. 418–428, 2014.

[17] S. J. Thomas, E. Wheeler, and J. Teizer, "Quadrature amplitude modulated backscatter in passive and semipassive UHF RFID systems," *IEEE Transaction on Microwave Theory and Techniques*, vol. 60, no. 4, pp. 1175–1182, 2012.

[18] G. Papotto, F. Carrara, A. Finocchiaro, and G. Palmisano, "A 90-nm CMOS 5-mbps crystal-less RF-powered transceiver for wireless sensor network nodes," *IEEE Journal of Solid-State Circuits*, vol. 49, no. 2, pp. 335–346, 2014.

[19] C. Ok, H. Thadakamalla, and U. Raghavan, "Optimal transmission power in self-sustainable sensor networks for pipeline monitoring," in *2007 IEEE International Conference on Automation Science and Engineering*, Scottsdale, AZ, USA, 2007.

[20] X. Lu, P. Wang, D. Niyato, D. I. Kim, and Z. Han, "Wireless networks with RF energy harvesting: a contemporary survey," *Networking and Internet Architecture*, 2014, http://arxiv.org/abs/1406.6470.

[21] L. Xia, J. Cheng, N. E. Glover, and P. Chiang, "0.56 V, −20 dBm RF-powered, multi-node wireless body area network system-on-a-chip with harvesting-efficiency tracking loop," *IEEE Journal of Solid-State Circuits*, vol. 49, no. 6, pp. 1345–1355, 2014.

[22] S. Agrawal, S. K. Pandey, J. Singh, and M. S. Parihar, "Realization of efficient RF energy harvesting circuits employing different matching technique," in *2014 15th International Symposium on Quality Electronic Design (ISQED)*, pp. 754–761, Santa Clara, CA, USA, March, 2014.

[23] S. Leng, D. W. K. Ng, and R. Schober, "Power efficient and secure multiuser communication systems with wireless information and power transfer," in *2014 IEEE International Conference on Communications Workshops (ICC)*, Sydney, Australia, June, 2014.

[24] A. Seyedi and B. Sikda, "Energy efficient transmission strategies for body sensor networks with energy harvesting," *Transactions on Communications*, vol. 58, no. 7, pp. 2116–2126, 2010.

[25] H. P. Tan, P. W. Lee, W. K. Seah, and Z. A. Eu, "Impact of power control in wireless sensor networks powered by ambient energy harvesting (WSN-HEAP) for railroad health monitoring," in *WAINA '09. International Conference on Advanced Information Networking and Applications Workshops*, Bradford, UK, May 2009.

[26] D. M. Dobkin, *The RF in RFID: Passive UHF RFID in Practice*, Burlington, MA: Newnes, USA, 2008.

[27] T. S. Ajitha and V. Bhanumathi, "Improving RFID tag efficiency by QAM backscatter modulation," *International Journal of Scientific & Engineering Research*, vol. 4, no. 4, pp. 421–427, 2013.

[28] L. Burgess, "FCC and ETSI requirements for short-range UHF ASK modulated transmitters," *High Frequency Electronics*, vol. 12, pp. 28–35, 2005.

[29] R. Gonsalves, "Evaluation of outage probability in two-tier open access femtocell networks," in *2014 International Conference on Circuits, Systems, Communication and Information Technology Applications (CSCITA)*, Mumbai, India, April 2014.